IUPAC Task Group on Atmospheric Chemical Kinetic Data Evaluation – Data Sheet HOx_VOC54

The citation for this data sheet is: IUPAC Task Group on Atmospheric Chemical Kinetic Data Evaluation, (http://iupac.pole-ether.fr)

This datasheet last evaluated: December 2019; last change in preferred values: December 2019

$$HO_2 + CH_3C(O)O_2 \rightarrow O_2 + CH_3C(O)OOH \quad (1)$$
$$\rightarrow O_3 + CH_3C(O)OH \quad (2)$$
$$\rightarrow O_2 + HO + CH_3C(O)O \quad (3)$$

$\Delta H°(1) = -180$ kJ·mol^{-1}
$\Delta H°(2) = -132$ kJ·mol^{-1}
$\Delta H°(3) = -13$ kJ·mol^{-1}

Rate coefficient data ($k = k_1 + k_2 + k_3$)

k/cm^3 molecule^{-1} s^{-1}	Temp./K	Reference	Technique/ Comments
Absolute Rate Coefficients			
$4.3 \times 10^{-13} \exp[(1040 \pm 100)/T]$	253-368	Moortgat et al., 1989	FP-AS (a)
$(1.3 \pm 0.3) \times 10^{-11}$	298		
$3.9 \times 10^{-13} \exp[(1350 \pm 250)/T]$	269-363	Crawford et al., 1999	PLP-IR-AS (b)
$(4.4 \pm 1.6) \times 10^{-11}$	297		
$6.4 \times 10^{-13} \exp[(925 \pm 120)/T]$	273-403	Tomas et al., 2001	FP-AS (c)
$(1.51 \pm 0.07) \times 10^{-11}$	293		
$(1.50 \pm 0.08) \times 10^{-11}$	293	Le Crâne et al., 2006	FP-AS (d)
$(1.4 \pm 0.5) \times 10^{-11}$	298	Dillon and Crowley, 2008	PLP-LIF (e)
$(2.1 \pm 0.4) \times 10^{-11}$	298*	Groß et al., 2014	PLP-LIF-AS (f)
$(2.4 \pm 0.4) \times 10^{-11}$	293	Winiberg et al., 2016	UVP-FTIR-LIF (g)
$1.38 \times 10^{-12} \exp[(730 \pm 170)/T]$	228.9-294	Hui et al., 2019	PLP-IR-UVA (h)
$(1.72 \pm 0.22) \times 10^{-11}$	294		
Branching Ratios			
$k_1/k_2 \approx 3$	298	Niki et al., 1985	FTIR (i)
$k_2/k = 0.33 \pm 0.07$	253-368	Moortgat et al., 1989	FP-AS (j)
$k_1/k_2 = 3.3 \times 10^2 \exp[(-1430 \pm 480/T)]$	263-333	Horie and Moortgat, 1992	FTIR (k)
$k_1/k_2 = 2.7$	298		
$k_2/k = 0.12 \pm 0.04$	295	Crawford et al., 1999	PLP-FTIR (l)
$k_2/k = 0.20 \pm 0.02$	298-373	Tomas et al., 2001	FP-AS (m)
$k_1/k = 0.40 \pm 0.16$	298	Hasson et al., 2004	UVP-FTIR/HPLC (n)
$k_2/k = 0.20 \pm 0.08$			
$k_3/k = 0.40 \pm 0.16$			
$k_2/k = 0.20 \pm 0.01$	298	Le Crâne et al., 2006	FP-AS (o)
$k_3/k < 0.1$			
$k_1/k = 0.38 \pm 0.13$	296	Jenkin et al., 2007	UVP-FTIR (p)
$k_2/k = 0.12 \pm 0.04$			
$k_3/k = 0.43 \pm 0.10$			
$k_3/k = 0.5 \pm 0.2$	298	Dillon and Crowley, 2008	PLP-LIF (e)
$k_2/k = 0.16 \pm 0.08$	298*	Groß et al., 2014	PLP-LIF-AS (f)
$k_3/k = 0.61 \pm 0.09$			
$k_1/k = 0.37 \pm 0.10$	293	Winiberg et al., 2016	UVP-FTIR-LIF (g)
$k_2/k = 0.12 \pm 0.04$			
$k_3/k = 0.51 \pm 0.12$			
$k_2/k = 0.23 \pm 0.07$	294	Hui et al. 2019	PLP-IR-UVA (h)
$k_3/k = 0.48 \pm 0.09$			

$k_2/k = 0.22 \pm 0.06$	292.7
$k_3/k = 0.45 \pm 0.07$	
$k_2/k = 0.25 \pm 0.07$	280.1
$k_3/k = 0.44 \pm 0.07$	
$k_2/k = 0.28 \pm 0.08$	270.6
$k_3/k = 0.40 \pm 0.07$	
$k_2/k = 0.31 \pm 0.08$	259.3
$k_3/k = 0.39 \pm 0.08$	
$k_2/k = 0.40 \pm 0.13$	250.4
$k_3/k = 0.35 \pm 0.08$	
$k_2/k = 0.42 \pm 0.13$	240.1
$k_3/k = 0.32 \pm 0.09$	
$k_2/k = 0.45 \pm 0.13$	228.9
$k_3/k = 0.29 \pm 0.09$	

Comments

(a) Flash photolysis of Cl_2 in the presence of CH_3CHO-CH_3OH-N_2 mixtures at total pressures of 800 mbar to 866 mbar (600 Torr to 650 Torr). [$CH_3C(O)O_2$] was monitored by UV absorption over the wavelength range 195 nm to 280 nm and the absorption cross-section measured relative to $\Delta(HO_2) = 5.3 \times 10^{-18}$ cm^2 molecule^{-1} at 210 nm. Rate coefficients were derived from a computer simulation of absorption traces at a range of wavelengths, based on a mechanism including secondary removal of $CH_3C(O)O_2$. The mechanism assumed that the $CH_3C(O)O_2 + HO_2$ reaction proceeds by channels (1) and (2).

(b) Pulsed laser photolysis of Cl_2-CH_3OH-CH_3CHO-O_2-N_2 mixtures at a total pressure of about 67 mbar (50 Torr). The progress of the reaction was followed by time-resolved UV absorption measurements over the range 200 nm to 300 nm and by monitoring [HO_2] by infrared laser diode absorption at 1117.5 cm^{-1}. Because of the difficulty of deconvoluting the UV spectra, values of k were determined from the infrared measurements by fitting the [HO_2] profiles using a detailed mechanism. The mechanism assumed that the $CH_3C(O)O_2 + HO_2$ reaction proceeds by channels (1) and (2).

(c) Flash photolysis of Cl_2-CH_3CHO-CH_3OH-O_2-N_2 mixtures. The progress of the reaction was followed by time-resolved UV absorption measurements at 207 nm and 250 nm. Values of k were derived by simulation of the absorption measurements at 207 nm, using a detailed chemical mechanism. The mechanism assumed that the $CH_3C(O)O_2 + HO_2$ reaction proceeds by channels (1) and (2).

(d) Re-evaluation of the room temperature results of Tomas et al. (2001) using cross-sections recommended by Tyndall et al. (2001), with the assumption that the $CH_3C(O)O_2 + HO_2$ reaction proceeds by channels (1) and (2). Inclusion of channel (3) in the reaction mechanism, with $k_3/k = 0.4$, resulted in an optimised $k = (2.20 \pm 0.07) \times 10^{-11}$ cm^3 molecule^{-1} s^{-1}, but a stated poorer description of the data.

(e) Pulsed laser photolysis of Cl_2-CH_3CHO-CH_3OH-O_2-N_2 mixtures to generate the reagent radicals with HO_2 in large excess. The production and removal of HO radicals, formed in channel (3), was followed using direct detection by LIF. k and k_3/k were determined simultaneously from simulation of the time dependence of the HO radical concentration, using a detailed chemical mechanism. No systematic dependence on total pressure over the range 100 to 705 mbar was observed.

(f) Pulsed laser photolysis of Cl_2-CH_3CHO-CH_3OH-O_2-N_2 mixtures at room temperature. Experiments performed with initial [HO_2]/[$CH_3C(O)O_2$] in the range 0.9-47.0 at total pressures over the range 133 to 677 mbar, with the time dependence of the reagent radical concentrations monitored using UV absorption. The formation of O_3 (by channel (2)) and HO radicals (by channel (3)) was monitored using UV absorption and LIF, respectively. k, k_2/k and k_3/k were determined from simulation of the system using a detailed mechanism, with the errors in the optimised parameters assessed using a Monte Carlo approach. Values of k_3/k of 0.63 ± 0.09, 0.60 ± 0.09, and 0.54 ± 0.08 reported at 133, 266 and 677 mbar, respectively, with the final reported value tabulated

above based on the mean of all determinations. The reaction of $CH_3C(O)O_2$ with DO_2 was also investigated at 133 and 266 mbar by substituting the reagent CH_3OH with CH_3OD, leading to an identical value of k, but a larger value of $k_3/k = (0.80 \pm 0.14)$.

(g) UV irradiation of Cl_2-CH_3CHO-CH_3OH-air mixtures in a stainless steel chamber at a total pressure of 1 bar. The chamber was equipped with an FTIR detection system for organic reagents and products and O_3, and a LIF based FAGE system for detection of HO and HO_2. Experiments were performed with HO_2 in excess over $CH_3C(O)O_2$ ($[CH_3OH]/[CH_3CHO]$ in the range 1.5-5.6) and the initial time development of the system (< 50% depletion of CH_3CHO) was characterised. Values of k, k_1/k, k_2/k and k_3/k were derived simultaneously from optimised simulation of the system over the range of studied conditions using a detailed chemical mechanism.

(h) Pulsed laser photolysis of Cl_2-CH_3CHO-CH_3OH-O_2-N_2 mixtures at 133 mbar (100 Torr) total pressure. Initial concentration ratios, $[HO_2]/[CH_3C(O)O_2]$, varied in the range 1.3 – 4.8. HO_2 and HO monitored in the near IR and mid IR, respectively, in back-to-back experiments, using tuned TDL sources. Simultaneous UV monitoring at either 225 nm or 250 nm in the back-to-back experiments, such that the UV signals contained different contributions from $CH_3C(O)O_2$ and HO_2, and from the absorbing products formed (particularly O_3 and CH_3O_2). Values of k, k_2/k and k_3/k were optimised from simulation of the IR and UV transient decay traces, using a detailed chemical mechanism.

(i) FTIR study of irradiated Cl_2-HCHO-CH_3CHO-O_2 mixtures. The branching ratio was based on the analysis of the products $CH_3C(O)OOH$, $CH_3C(O)OH$ and O_3, with the assumption that the reaction proceeds via channels (1) and (2).

(j) Derived from the same experiments as in Comment (a) by making allowance for absorption by O_3 product.

(k) FTIR study of irradiated $CH_3C(O)C(O)CH_3$ in the presence of Ar-O_2 mixtures at total pressures of 973 mbar to 1026 mbar (730 Torr to 770 Torr). The reaction products CO_2, CO, HCHO, HCOOH, $CH_3C(O)OH$, $CH_3C(O)OOH$, CH_3OH, H_2O_2 and O_3 were analysed by matrix-isolation FTIR spectroscopy combined with a molecular-beam sampling technique. The branching ratio, k_1/k_2, was derived from the yields of $CH_3C(O)OOH$ and O_3 which are believed to be formed uniquely from channels (1) and (2) respectively.

(l) UV irradiation of Cl_2-CH_3CHO-CH_3OH-air mixtures in a smog chamber fitted with an FTIR detection system. Branching ratios were derived from the yields of $CH_3C(O)OOH$ and $CH_3C(O)OH$ which gave $k_2/k = 0.10 \pm 0.02$ at 295 K. Branching ratios were also derived from the O_3 yields determined from the kinetics traces at long reaction times in experiments performed to obtain the rate coefficient [see Comment (b)]. These experiments gave $k_2/k = 0.16 \pm 0.04$ at 295 K. The value cited in the Table is a weighted mean of values from all of the experiments. The O_3 yield measurements suggest only a small increase in k_2/k as temperature is lowered from 359 K to 265 K.

(m) Branching ratio was derived from the residual absorption at 240 nm (attributed to O_3) at long reaction times in experiments described in Comment (c). There was no detectable change in k_2/k with change in temperature from 298 K to 373 K.

(n) Continuous photolysis of Cl_2 in the presence of CH_3CHO-CH_3OH-O_2-N_2 mixtures at a total pressure of 1066 mbar (800 Torr). Yields of CH_3OOH and $CH_3C(O)OOH$ (by HPLC) and CH_3OOH, $CH_3C(O)OOH$, $CH_3C(O)OH$ and CO_2 (by FTIR) were measured as a function of the initial concentration ratio $[CH_3OH]_0/[CH_3CHO]_0$ over the range 0 to 5, corresponding to conditions over which dominant removal of $CH_3C(O)O_2$ changes from its self reaction to the reaction with HO_2. The results were analysed by simulation using a detailed chemical mechanism taking account of the sequential formation of CH_3O_2 in the system. A value of $k = 2.2 \times 10^{-11}$ cm^3 molecule^{-1} s^{-1} reported to provide the best description of the data in conjunction with the reported final branching ratios.

(o) Flash photolysis of Cl_2-CH_3CHO-CH_3OH-O_2-N_2 mixtures. Channel (3) was investigated through addition of benzene to scavenge HO, using absorption of the product HOC_6H_6 radicals at 290 nm as the diagnostic. Upper limit value of k_3/k determined from simulation of the kinetic absorption

traces at 290 nm using a detailed chemical mechanism. k_2/k was derived from the residual absorption at 240 nm (attributed to O_3) at long reaction times in the absence of benzene, with the assumption that the $CH_3C(O)O_2 + HO_2$ reaction proceeds by channels (1) and (2).

(p) UV irradiation of Cl_2-CH_3CHO-CH_3OH-air mixtures in a smog chamber fitted with an FTIR detection system, at a total pressure of 930 mbar. Channel (3) was investigated through addition of variable quantities of benzene to scavenge HO, using the formation of phenol as the diagnostic, based on a phenol yield of 0.531 ± 0.066 (Volkamer et al., 2002). k_1/k, k_2/k and k_3/k derived from optimised simulation of $CH_3C(O)OOH$, $CH_3C(O)OH$ and phenol formation, respectively, for a range of conditions, using a detailed chemical mechanism. Additional evidence for production of HO in the system was derived from examination of the relative removal of the reagents, CH_3CHO and CH_3OH, as a function of [benzene].

Preferred Values

Parameter	Value	T/K
k	2.0×10^{-11} cm^3 molecule^{-1} s^{-1}	298
k	1.73×10^{-12} exp(730/T) cm^3 molecule^{-1} s^{-1}	230-300
k_1/k	0.37	298
k_2/k	0.13	298
k_3/k	0.50	298
k_1	1.50×10^{-12} exp(480/T) cm^3 molecule^{-1} s^{-1}	230-300
k_2	4.40×10^{-15} exp(1910/T) cm^3 molecule^{-1} s^{-1}	230-300
k_3	4.66×10^{-12} exp(235/T) cm^3 molecule^{-1} s^{-1}	230-300
Reliability		
$\Delta \log k$	± 0.2	298
$\Delta E/R$	± 300 K	
$\Delta k_1/k$	± 0.1	298
$\Delta k_2/k$	± 0.1	298
$\Delta k_3/k$	± 0.1	298
$\Delta (E_1/R)$	± 300 K	
$\Delta (E_2/R)$	± 500 K	
$\Delta (E_3/R)$	± 300 K	

Comments on Preferred Values

The present evaluation adopts the approach reported recently by Jenkin et al. (2019). The preferred value of E/R = -730 K is taken from the recent study of Hui et al. (2019), the first to measure the temperature dependence of the reaction with HO recycling via channel (3) fully accounted for in the analysis. The preferred value of k at 298 K is based on an average of the more recent room temperature determinations of Groß et al. (2014), Winiberg et al. (2016) and Hui et al. (2019) (corrected to 298 K where necessary using the preferred value of E/R), and the pre-exponential factor is set to return the 298 K value of k. The measurements of k in earlier temperature dependence studies (Atkinson et al., 2006; and references therein) are expected to be subject to systematic errors, because reagent radical regeneration via channel (3) was not taken into account in the analyses. Those studies therefore generally report stronger temperature dependences than that reported by Hui et al. (2019).

The contribution of the propagating channel (3) has been quantified at 293-298 K in a number of more recent studies (Hasson et al., 2004; Jenkin et al., 2007; Dillon and Crowley, 2008; Groß et al., 2014; Winiberg et al., 2016; Hui et al., 2019), and a value of $k_3/k = 0.5$ is assigned at 298 K, based on the average of these determinations. The participation of the terminating channels (1) and (2) is very well established. Reasonably consistent branching ratios (k_1/k_2), lying in the approximate range 2–3 at room temperature, have been reported in studies where products of both channels have been measured (Niki et al., 1985; Horie and Moortgat, 1992; Hasson et al., 2004; Jenkin et al., 2007; Winiberg et al., 2016), with an average value of 2.8. In conjunction with the above value of $k_3/k = 0.5$, this results in $k_1/k = 0.37$ and $k_2/k = 0.13$ at 298 K, as also recommended in our previous evaluation.

The temperature dependence of k_3/k is based on that reported in the recent study of Hui et al. (2019). The temperature dependences of k_1/k and k_2/k are derived from the experimental characterization of k_1/k_2 reported by Horie and Moortgat (1992) (adjusted slightly to return the relative value at 298 K indicated above), leading to $k_1/k_2 = 3.4 \times 10^2 \exp(-1430/T)$, as recommended in our previous evaluation. Fitting Arrhenius expressions to the resultant data over the temperature range 230-300 K results in the preferred individual channel rate coefficients tabulated above. The use of these expressions results in the branching ratios illustrated below, which are compared with those reported in studies which take account of channel (3) in the analysis. As also shown below, the total rate coefficients obtained by summing the three expressions agree with the recommended expression for the overall rate coefficient to within 5 % over the temperature range 230-300 K, although larger deviations would occur if they are applied outside this recommended temperature range.

References

Atkinson, R., Baulch, D. L., Cox, R. A., Crowley, J. N., Hampson, R. F., Hynes, R. G., Jenkin, M. E., Rossi, M. J., and Troe, J.: Atmos. Chem. Phys., 6, 3625, https://doi.org/10.5194/acp-6-3625-2006, 2006.

Crawford, M. A., Wallington, T. J., Szente, J. J., Maricq, M. M. and Francisco, J. S.: J. Phys. Chem. A, 103, 365, 1999.

Dillon, T. J. and Crowley, J. N.: Atmos. Chem. Phys., 8, 4877, 2008.

Groß, C. B. M., Dillon, T. J., Schuster, G., Lelieveld, J., and Crowley, J. N.: J. Phys. Chem. A, 118, 974–985, doi:10.1021/jp412380z, 2014.

Hasson, A. S., Tyndall, G. S. and Orlando, J. J.: J. Phys. Chem. A, 108, 5979, 2004.

Horie, O. and Moortgat, G. K.: J. Chem. Soc. Faraday Trans., 88, 3305, 1992.

Hui, A. O., Fradet, M., Okumura, M., and Sander, S. P.: J. Phys. Chem. A, 123 (17), 3655, doi: 10.1021/acs.jpca.9b00442, 2019.

Jenkin, M. E., Hurley, M. D. and Wallington, T. J.: Phys. Chem. Chem. Phys., 9, 3149, 2007.

Jenkin, M. E., Valorso, R., Aumont, B., and Rickard, A. R.: Atmos. Chem. Phys., 19, 7691, https://doi.org/10.5194/acp-19-7691-2019, 2019.

Le Crâne, J-P., Rayez, M-T, Rayez, J-C. and Villenave, E.: Phys. Chem. Chem. Phys., 8, 2163, 2006.

Moortgat, G. K., Veyret, B. and Lesclaux, R.: Chem. Phys. Lett., 160, 443, 1989.

Niki, H., Maker, P. D., Savage, C. M. and Breitenbach, L. P.: J. Phys. Chem. 89, 588, 1985.

Tomas, A., Villenave, E. and Lesclaux, R.: J. Phys. Chem. A, 105, 3505, 2001.

Tyndall, G. S., Cox, R. A., Granier, C., Lesclaux, R., Moortgat, G. K., Pilling, M. J., Ravishankara, A. R. and Wallington, T. J.: J. Geophys. Res., 106, 12157, 2001.

Volkamer, R., Klotz, B., Barnes, I., Imamura, T., Wirtz, K., Washida, N., Becker, K. H. and Platt, U.: Phys. Chem. Chem. Phys., 4, 1598, 2002.

Winiberg, F. A. F., Dillon, T. J., Orr, S. C., Groß, C. B. M., Bejan, I., Brumby, C. A., Evans, M. J., Smith, S. C., Heard, D. E., and Seakins, P. W.: Atmos. Chem. Phys., 16, 4023-4042, doi:10.5194/acp-16-4023-2016, 2016.

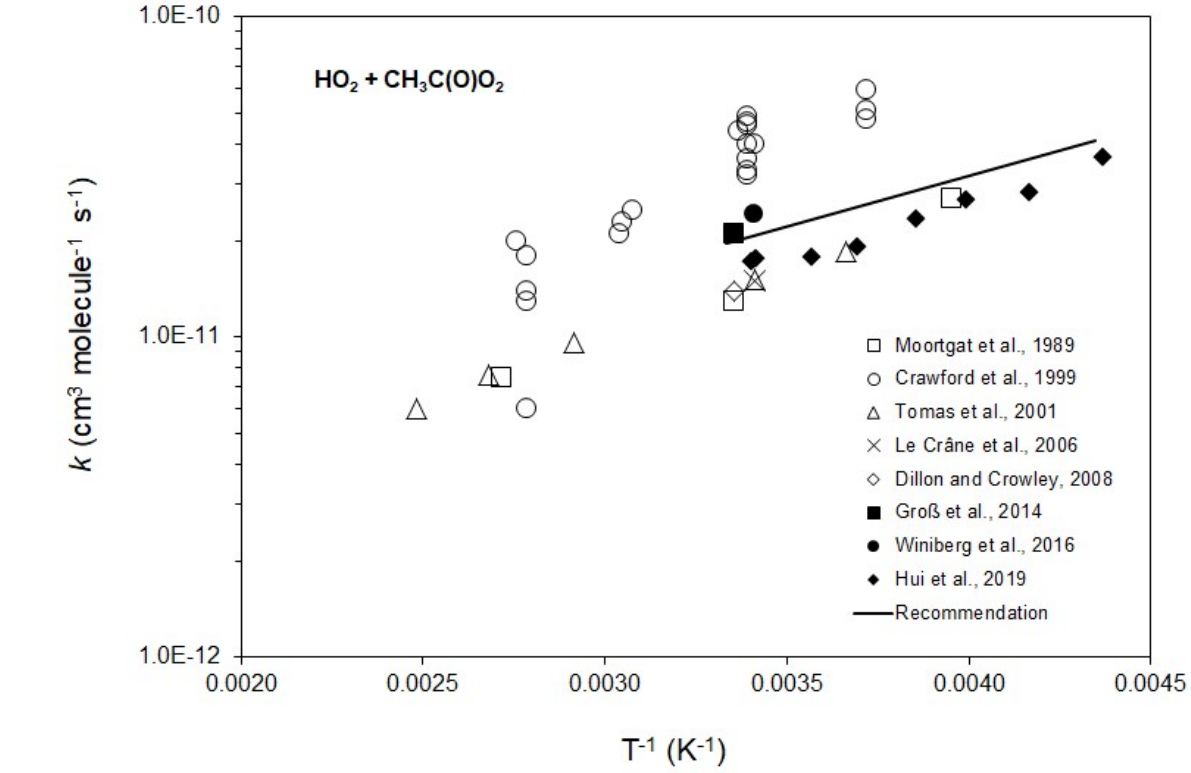

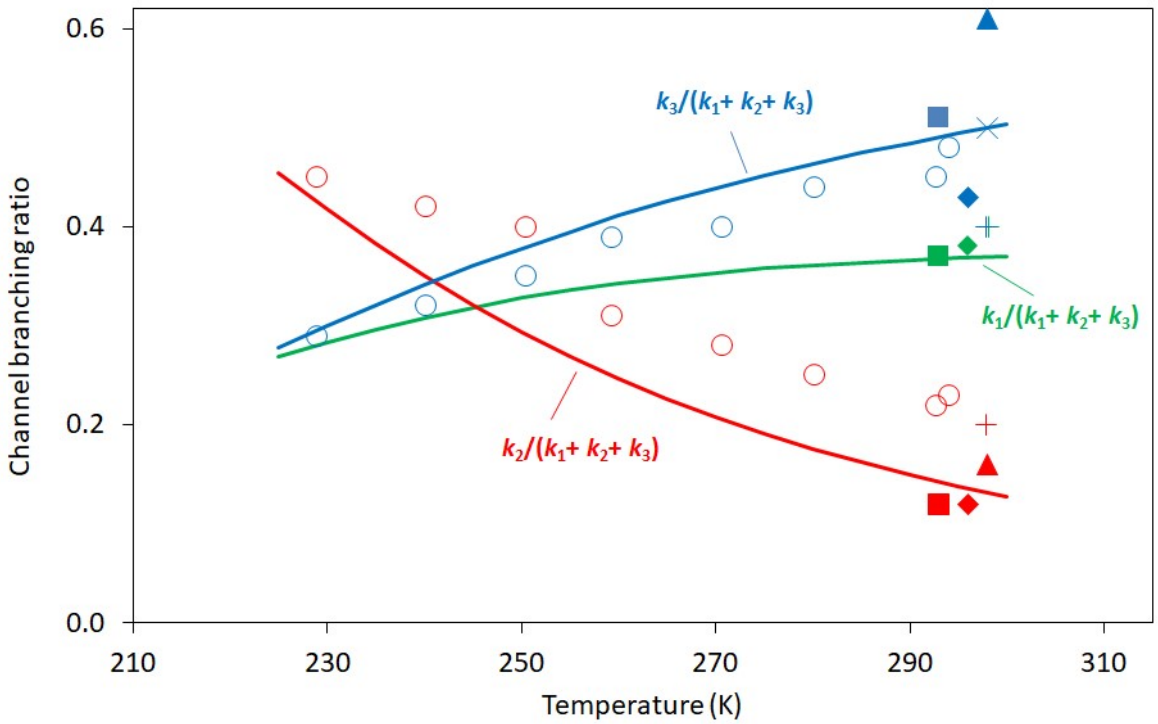

Product channel branching ratios reported for k_1/k (green points), k_2/k (red points) and k_3/k (blue points) in studies taking account of channel (3): Hasson et al. (2004) (+); Jenkin et al. (2007) (diamonds); Dillon and Crowley (2008) (×);Groß et al. (2014) (triangles); Winiberg et al. (2016) (squares); Hui et al. (2019) (circles). The solid lines represent the corresponding ratios, based on the individual Arrhenius expressions for k_1, k_2 and k_3, as tabulated in the preferred values.

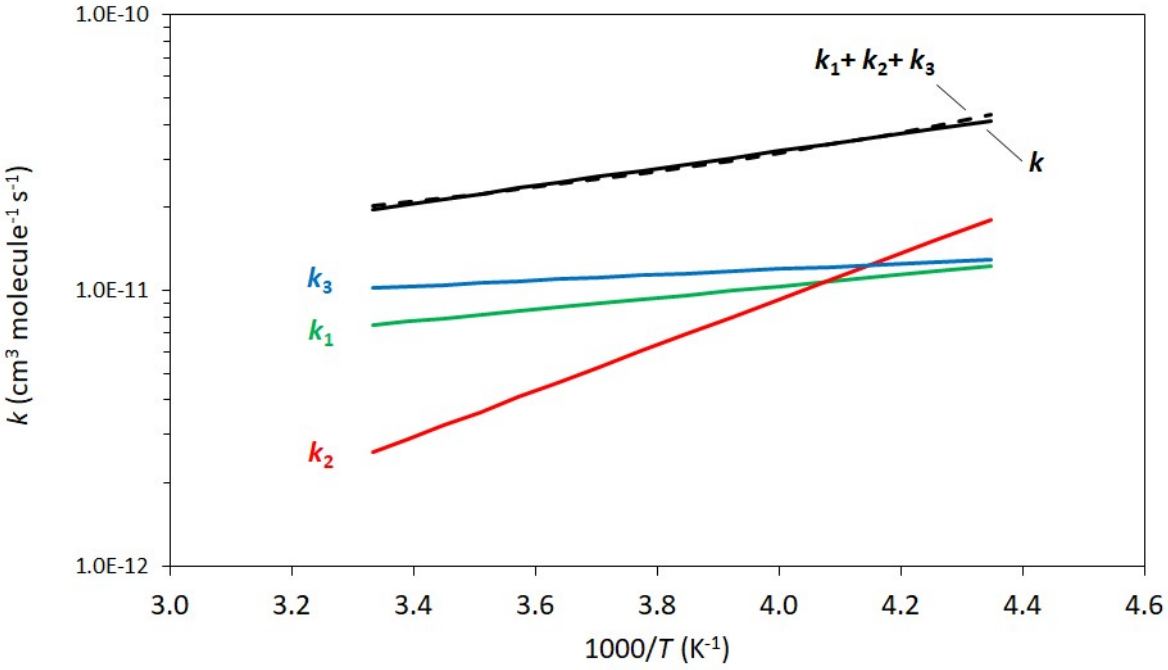

Illustration of the recommended temperature dependence for k (solid black line); and those for the individual reaction channels, k_1, k_2 and k_3, as tabulated in the preferred values. The black broken line shows the total values derived from summing the individual expressions for k_1, k_2 and k_3.